Biochimica et Biophysica Acta 1833 (2013) 3166–3175

Contents lists available at ScienceDirect

Biochimica et Biophysica Acta

journal homepage: www.elsevier.com/locate/bbamcr

Identification of voltage-gated K^+ channel beta 2 (Kvβ2) subunit as a novel interaction partner of the pain transducer Transient Receptor Potential Vanilloid 1 channel (TRPV1)☆

Carlo Bavassano [a], Letizia Marvaldi [b], Michiel Langeslag [c], Bettina Sarg [d], Herbert Lindner [d], Lars Klimaschewski [b], Michaela Kress [c], Antonio Ferrer-Montiel [e], Hans-Günther Knaus [a,*]

[a] Division of Cellular and Molecular Pharmacology, Medical University Innsbruck, Peter-Mayr strasse 1, 6020 Innsbruck, Austria
[b] Division of Neuroanatomy, Medical University Innsbruck, Müllerstrasse 59, 6020 Innsbruck, Austria
[c] Division of Physiology, Medical University Innsbruck, Fritz-Pregl-Straße 3, 6020 Innsbruck, Austria
[d] Division of Clinical Biochemistry, Medical University Innsbruck, Innrain 80, 6020 Innsbruck, Austria
[e] IBMC, Universidad Miguel Hernandez Elche, Av. de la Universidad s/n., Edif. Torregaitán, E-03202, Spain

ARTICLE INFO

Article history:
Received 20 June 2013
Received in revised form 2 September 2013
Accepted 3 September 2013
Available online 11 September 2013

Keywords:
Signaling complex
Dorsal root ganglia
Accessory subunit
TRPV1

ABSTRACT

The Transient Receptor Potential Vanilloid 1 (TRPV1, vanilloid receptor 1) ion channel plays a key role in the perception of thermal and inflammatory pain, however, its molecular environment in dorsal root ganglia (DRG) is largely unexplored. Utilizing a panel of sequence-directed antibodies against TRPV1 protein and mouse DRG membranes, the channel complex from mouse DRG was detergent-solubilized, isolated by immunoprecipitation and subsequently analyzed by mass spectrometry. A number of potential TRPV1 interaction partners were identified, among them cytoskeletal proteins, signal transduction molecules, and established ion channel subunits. Based on stringent specificity criteria, the voltage-gated K^+ channel beta 2 subunit (Kvβ2), an accessory subunit of voltage-gated K^+ channels, was identified of being associated with native TRPV1 channels. Reverse co-immunoprecipitation and antibody co-staining experiments confirmed TRPV1/Kvβ2 association. Biotinylation assays in the presence of Kvβ2 demonstrated increased cell surface expression levels of TRPV1, while patch-clamp experiments resulted in a significant increase of TRPV1 sensitivity to capsaicin. Our work shows, for the first time, the association of a Kvβ subunit with TRPV1 channels, and suggests that such interaction may play a role in TRPV1 channel trafficking to the plasma membrane.

1. Introduction

TRPV1 is a Ca^{2+} and Na^+-permeable ion channel responding to heat (>42 °C), acidosis (pH < 6), endovanilloids and a variety of chemicals of which capsaicin, the pungent component of red hot chili, is best known [1,2]. This ion channel is predominantly expressed in the peripheral sensory system, and therefore is in a strategic position to determine specificity, speed and modulation of sensory and nociceptive neurotransmission [2]. TRPV1 channels are associated with inflammatory pain and thermal hyperalgesia [3]: mice lacking TRPV1 channels are impaired in the detection of noxious heat, and show impaired thermal hypersensitivity [3].

TRPV1 is the ancestor of the transient receptor potential vanilloid channel family, which structurally resembles voltage-gated potassium channels [4]. Accordingly, these channels are presumed to be constituted of four identical subunits, each of which having six membrane-spanning domains (S1–S6) and intracellular carboxyl and amino termini [1].

Recent research indicates that many ion channels are organized in a multiprotein assembly, termed signaling complexes, where channel regulation is critically dependent on protein–protein interactions [5]. For instance, proteomic studies on NMDA receptors, or voltage-gated calcium channels, demonstrated close interaction of multiple polypeptides which modulate the ion channel function, some of which have previously not been identified of being associated with ion channels [6,7].

Abbreviations: AKAP, A kinase anchor protein; ATP, adenosine tris-phosphate; BSA, bovine serum albumin; cDNA, complementary deoxyribonucleic acid; CHAPS, 3-[(3-cholamidopropyl)dimethylammonio]-1-propanesulfonate; CHO, Chinese hamster ovary; CGRP, calcitonin gene-related peptide; CMC, critical micelle concentration; DAPI, 4′,6-diamidino-2-phenylindole; DNA, deoxyribonucleic acid; DRG, dorsal root ganglia; DTT, di-tiothreitol; EDTA, ethylenediaminetetraacetic acid; EGTA, ethylene glycol tetraacetic acid; GAPDH, glyceraldehyde-3-phosphate dehydrogenase; HEPES, 4-(2-hydroxyethyl)-1-piperazineethanesulfonic acid; Kvβ2, voltage-gated K^+ channel subunit beta 2; Icaps, capsaicin-activated current; IgG, immunoglobulin G; PMSF, phenylmethylsulfonyl fluoride; PBS, phosphate buffer saline; SDS, sodium dodecyl sulfate; TRPV1, Transient Receptor Potential Vanilloid 1; WT mouse, wild type mouse

☆ This work was supported by the Austrian Research Foundation PhD program SPIN B05, Project Number ZFW1206-05.

* Corresponding author. Tel.: +43 512 9003 70440; fax: +43 512 9003 73440.
E-mail addresses: carlo.bavassano@i-med.ac.at (C. Bavassano), letizia.marvaldi@i-med.ac.at (L. Marvaldi), michiel.langeslag@i-med.ac.at (M. Langeslag), bettina.sarg@i-med.ac.at (B. Sarg), herbert.lindner@i-med.ac.at (H. Lindner), lars.klimaschewski@i-med.ac.at (L. Klimaschewski), michaela.kress@i-med.ac.at (M. Kress), aferrer@umh.es (A. Ferrer-Montiel), hans.g.knaus@i-med.ac.at (H.-G. Knaus).

0167-4889/$ – see front matter © 2013 Elsevier B.V. All rights reserved.
http://dx.doi.org/10.1016/j.bbamcr.2013.09.001

Recombinant TRPV1 channels retain functional properties similar to those of their native counter-parts, for instance, from sensory neurons [8]. However, the pharmacological profile of these recombinant channels differs from native channel, giving room for a possible co-association of accessory regulatory proteins in native channels [8]. Therefore, the peculiarity of TRPV1 channel signaling could be partly due to association of thus far uncharacterized proteins. In this context, a limited number of previous studies focused on protein–protein interaction of the pore-forming subunit TRPV1 with potential interaction partners [9–15]. For instance, tubulin was shown to be capable to associate with TRPV1 protein [9,10], demonstrating direct association of TRPV1 with cytoskeletal elements. In addition, co-immunoprecipitation and co-staining experiments indicated an intimate and physiologically relevant interaction of TRPV1 with TRPV2 subunits in rodent dorsal root ganglia (DRG), as well as in cell lines after recombinant channel expression [12,14]. The protein kinase A anchoring protein 150 (AKAP150) and the phosphoinositide-binding protein Pirt were also found to associate with TRPV1 channels [11,15]. The alternative approach of yeast two-hybrid screening identified two interacting proteins, snapin and synaptotagmin IX, which play a role in SNARE-dependent exocytosis, suggesting that their interaction with TRPV1 may modulate aspects of TRPV1 trafficking and/or delivery to the plasma membrane [13].

In order to deepen our insight into TRPV1 channel assembly, we embarked on a systematic approach of isolating native TRPV1 channel complexes through immunoprecipitation with anti-TRPV1 antibodies and identifying the isolated complex components by mass spectrometry. We report the identification of the voltage-gated K^+ channel accessory subunit beta 2 (Kvβ2) as a novel TRPV1 interacting protein. Thus far, Kvβ2 was believed to be an exclusive ancillary subunit of voltage-gated K^+ channels (Kv) which is associated with a cytoplasmic domain on pore-forming Kv1 (Shaker) alpha subunits [16]. Their functional contribution was shown to be either conferring an inactivation particle to the Kv1 channel family [17], or facilitating the trafficking of the Kv1 channel to the plasma membrane [18]. This is the first study that demonstrates that Kvβ2 is found in association with structurally different pore-forming subunits other than Kv channels.

2. Experimental procedures

2.1. Reagents

For immunoprecipitation experiments, two polyclonal sera were raised and affinity purified as previously published [19]. The sequences of the synthetic peptides employed and their location along the rat TRPV1 sequence are: EDA EVF KDS MVP GEK (anti-TRPV1$_{(824–838)}$) and EDP GNC EGV KRT LSF SLR (anti-TRPV1$_{(761–778)}$). The amino acid numbering refers to the rat TRPV1 clone isoform 1 (accession number: O35433). An additional rabbit anti-TRPV1 antibody was purchased from Sigma-Aldrich, directed against amino acids 817–838 of rat and mouse TRPV1. This antibody was used for immunostaining and Western blotting experiments. Monoclonal anti-Kvβ2 antibody (clone K17/70) was purchased from NIH Neuromab. Monoclonal anti-c-*myc* (clone 9E10) was from Sigma-Aldrich. Monoclonal anti-GAPDH-hrp (clone GAPdh-71.1) was from Sigma-Aldrich. Monoclonal anti-Na^+/K^+ ATPase α1 (clone C464.6) was from Upstate Biotechnology.

Fluorescently-labeled secondary antibodies, anti-rabbit Alexa fluor-488 and anti-mouse Alexa fluor-594, were from Invitrogen. Anti-fade mounting media were from Vectashield. High glucose DMEM for cell culture, poly-L-lysine and laminin were from Sigma-Aldrich. Fetal bovine serum, trypsin–EDTA, L-glutamine, streptomycin sulfate, and protein A coated Dynabeads were from Invitrogen. Liberase Blendzyme 1 was from Roche. TNB medium and Protein–Lipid-Complex were from Biochrom. Streptavidin magnetic beads and Sulf-NHS-LC-LC-Biotin were from Thermo Scientific.

Primers for subcloning were from Sigma, pcDNA3.1 and pcDNA3 plasmids were from Invitrogen, and pGFP-c1 plasmid was from Clontech.

Dodecanoyl sucrose was purchased from Merck (Darmstadt, Germany), mass spectrometry grade trypsin from Promega, and cell transfection reagent Metafectene Pro was from Biontex.

2.2. Animals

TRPV1 deficient mice (TRPV1$^{-/-}$) were purchased by Charles River–Jackson Laboratories (strain B6.129X1-Trpv1^{tm1Ju}l/J). TRPV1$^{-/-}$ and C57Bl/6J wild type (WT) mice were housed and handled in accordance with the guidelines of the Directive 2010/63/EU for the use of laboratory animals.

2.3. Cell line culture

The mammalian cell line tsA201 is derived from human embryonic kidney HEK-293 cells by stable transfection with SV40 large-T antigen and has been reported to produce high levels of recombinant proteins [20]. N1E-115-1 cells are derived from mouse neuroblastoma and have been utilized in a wide range of functional studies [21]. tsA-201 cells were maintained at 37 °C and 5% CO_2 in high glucose DMEM supplemented with 10% (v/v) fetal bovine serum and 1% (v/v) penicillin/streptomycin (PAA). Cells were transiently transfected with Metafectene Pro following manufacturers's guidelines. N1E-115-1 cells were maintained and transfected in the same conditions used for tsA-201 cells.

2.4. DRG membrane preparation and TRPV1 complex solubilization

DRG membrane fraction was prepared according to Berkefeld et al. [22] with minor modifications. Briefly, whole DRG from adult mice were dissected and collected in PBS containing 3 mM EDTA and 0.5 mM PMSF. Subsequently, they were homogenized with a glass potter in lysis buffer (10 mM Tris pH7.4, 1 mM EDTA, 1 mM iodoacetamide, 1 mM PMSF and protease inhibitors: 2 μM leupeptin, 1.5 μM aprotinin and 0.15 μM pepstatin). Low-speed centrifugation (1000 ×*g*) was performed twice to remove cellular debris, resuspending the pellet in lysis buffer in between. The resulting supernatant was centrifuged at high-speed (100,000 ×*g*) 15 min, the membrane fraction pellet was resuspended in 20 mM Tris, and protein concentration was determined. In order to solubilize the TRPV1 protein complex, the membrane fraction was incubated in solubilization buffer (1% dodecanoyl sucrose (w/v), 150 mM NaCl, 20 mM Tris pH7.4, 1 mM EDTA, 1 mM PMSF and protease inhibitors, in the same concentration as mentioned above), 30 min on ice. Subsequent high-speed centrifugation (100,000 ×*g*) 30 min led to the separation of non-soluble pellet from a solubilized supernatant. This fraction was used as starting material for the immunoprecipitation experiment described below.

2.5. Immunoprecipitation of TRPV1 protein complex

Antibodies immobilized on protein A-coated Dynabeads were incubated with the detergent-solubilized membrane fraction obtained from mouse DRG (see above) 2 h at 4 °C. 10 μg of antibody was used to precipitate 300 μg of total membrane extract for analytical experiments. For mass spectrometric sequencing, 3 mg of total membrane protein was used as starting material. After immunoprecipitation, the TRPV1 complex was eluted under denaturing conditions (Laemmli buffer without reducing agent). Thereafter, reducing agent dithiothreitol (DTT) was added to the sample (final concentration of 120 mM). For MS-sequencing, eluates were shortly run on SDS-PAGE minigels, stained by silver staining [23], divided into three molecular-weight ranges and separately subjected to in-gel trypsin digestion according to Shevchenko et al. [24], with the only modification that the gel pieces were incubated overnight at 37 ° C with trypsin (5 μg/ml).

2.6. Mass spectrometric analysis

Protein digests were analyzed using an UltiMate 3000 nano-HPLC system (Dionex, Germering, Germany) coupled to an LTQ Orbitrap XL mass spectrometer (ThermoScientific, Bremen, Germany) equipped with a nanospray ionization source. A fritless fused silica microcapillary column (75 μm i.d. × 280 μm o.d.) packed with 10 cm of 3 μm reverse-phase C18 material (Reprosil) was used. The gradient (solvent A: 0.1% formic acid; solvent B: 0.1% formic acid in 85% acetonitrile) started at 4% B. The concentration of solvent B was increased linearly from 4% to 40% during 67 min and from 40% to 100% during 10 min. A flowrate of 250 nl/min was applied.

Mass Spectrometry (MS) instrument settings were as follows: Mass spectra were acquired in positive ion mode applying a data-dependent automatic switch between survey scan and MS/MS acquisition. Survey MS scans (from m/z 300 to 2000) were acquired in the Orbitrap with a resolution of R = 60,000; the target value was 200,000; maximum ionization time was set to 20 ms. Up to four of the most intense ions per scan were fragmented in the linear trap (LTQ) using collision induced dissociation (CID) at a target value of 10,000; the maximum ionization time was set to 100 ms. Dynamic exclusion settings: repeat count 1; repeat duration 50 s; exclusion duration was 45 s. Charge state screening was enabled; unassigned and singly charged ions were excluded from MS/MS.

Protein identification was performed using the Mascot search engine and the NCBInr database (*Mus musculus*) accepting variable modifications, carbamidomethyl (C), and oxidation (M). Specific cleavage sites for trypsin (KR) were selected with two missed cleavage sites allowed. Peptide tolerance was +20 ppm and MS/MS tolerance was +0.8 Da. We selected the candidate peptides with probability-based Mowse scores (total score) that exceeded its threshold indicating a significant homology ($P < 0.05$). Peptides with a Mascot score below 20 were skipped.

2.7. Primary sensory neuron culture

L1–L6 lumbar dorsal root ganglia (DRG) were dissected from adult mice as previously published [25]. After removal of connective tissue, ganglia were incubated in Liberase Blendzyme 1 (9 mg/100 ml DMEM) for 60 min. After rinsing with PBS, 1× trypsin–EDTA was added for 15 min and DRG were washed with TNB medium supplemented with L-glutamine, penicillin G sodium, streptomycin sulfate, and Protein–Lipid-Complex. DRG were dissociated with a fire-polished Pasteur pipette and centrifuged through a 3.5% BSA gradient to minimize non-neuronal cells. The sensory neurons were resuspended, plated on coverslips coated with poly-L-Lysine/laminin-1, and cultivated in TNB medium at 37 °C in 5% CO_2 for 24 h.

2.8. Immunocytochemistry and microscopy

Neurons were kept for 24 h in culture, fixed with 4% PFA for 20 min, permeabilized with 0.1% Triton X-100 (Sigma) 5 min and blocked with 10% goat serum in PBS for 30 min. Cells were incubated with primary antibodies against TRPV1 and Kvβ2 dissolved in 10% goat serum in PBS (1:4000 and 1:1000) respectively for 60 min at room temperature (RT), washed with PBS, and incubated with secondary antibodies (1:1000) for 30 min at RT. Nuclei were stained with 4′,6-diamidino-2-phenylindole (DAPI 1:1000 in PBS) and cells were embedded in mounting medium. Neurons were documented applying a Zeiss fluorescence microscope equipped with a SPOT RT digital camera. Neurons resulting positive both to TRPV1 and Kvβ2 staining were evaluated. Average cell fluorescence intensities were measured after background subtraction applying Metamorph software (MetaMorph®, version 7.5.6, Visitron Systems). For confocal microscopy, z-stack images were acquired with Leica SP5 confocal microscope, and analyzed with Huygens Professional image deconvolution software.

2.9. Molecular biology

Kvβ2 cDNA was kindly provided by J. Trimmer. Kvβ2 cDNA was subcloned in pGEMHE by digesting with *XbaI* and *ClaI*, both in the multiple cloning site, blunting both ends and subcloning into the SmaI site of pGEMHE. *BamHI* and *EcoRI* restriction sites were then attached respectively at the 5′ and 3′ ends of the coding sequence by PCR, and were used to subclone Kvβ2 into pcDNA3.1-*myc*-His plasmid. mTRPV1 cDNA cloned into pcDNA3 plasmid was provided by M. Caterina. For electrophysiology recording, TRPV1 plasmid was co-transfected with pGFP-C1 plasmid to identify TRPV1 expressing N1E-115-1 cells. The integrity of all constructs was confirmed by DNA sequencing (Secugen).

2.10. Co-immunoprecipitation in tsA-201 cell line

12×10^5 tsA-201 cells were seeded in 60 mm dishes 24 h before transfection. For each condition, 5 μg of total cDNA was transfected and equimolar amounts of cDNA were used in double transfection conditions. The amount of cDNA was kept constant by addition of empty pcDNA3 plasmid in mock and single transfection conditions. Cells were harvested 48 h after transfection, washed twice in PBS and lysated by mechanical trituration (27G syringe needle) in lysis buffer (same as described in the DRG membrane preparation section) on ice. Centrifugation steps, TRPV1 complex solubilisation and immunoprecipitation were as described for DRG membranes. The eluates were run on 9% SDS-PAGE minigels, blotted on PVDF membrane and monitored by Western analysis with rabbit anti-TRPV1 (0.1 μg/ml) and mouse anti-*myc* (1:5000) antibodies.

2.11. Electrophysiology

N1E-115-1 cells were used for electrophysiology 18 to 28 h after plating on 24 mm coverslips. Ionic currents were recorded in the classical whole-cell voltage-clamp configuration of the patch-clamp technique as previously published [21,26,27]. Calcium-free ECS contained: 150 mM NaCl, 5 mM KCl, 1 mM $MgCl_2$, 10 mM glucose, and 10 mM HEPES, at pH 7.3 adjusted with NaOH. Calcium was removed to avoid desensitization of capsaicin-induced currents. Borosilicate glass pipettes (Science Products) pulled with a horizontal puller (Sutter Instruments Company) were filled with internal solution (ICS): 148 mM KCl, 2 mM $MgCl_2$, 2 mM MgATP, 0.1 mM $CaCl_2$, 1 mM EGTA, and 10 mM HEPES, at pH 7.3 adjusted with KOH. After filling, electrode resistance was 2–4 MΩ. N1E-115-1 cells were recorded at 0 mV holding potential, and to monitor TRPV1 channel activation the cells were challenged by a 200 ms voltage ramp from −100 to +100 mV every 2.5 s. Currents were sampled at 50 kHz and filtered at 2.9 kHz, and recorded with an EPC10 (HEKA) and the Pulse v8.74 software (HEKA). A ten barrel system with common outlet was used for fast drug administration (WAS 02, Dittel, Prague). Capsaicin-activated currents (Icaps) were elicited by applying increasing concentrations of capsaicin (Sigma) for 10 s followed by a 60 s washout with control solution. Experiments were performed at room temperature and only a single N1E-115-1 cell was tested per coverslip. Capsaicin dose–response curves were fitted with a Boltzmann equation (Origin Pro 7, OriginLab).

$$I = Imax + \frac{Imin - Imax}{1 + e^{([Caps] - EC50)/d[Caps]}}$$

$$Slope = \frac{Imax - Imin}{4 * d[Caps]}$$

Mann–Whitney *U*-test was used to determine statistical significance.

2.12. Biotinylation assay

Biotinylation and isolation of transfected tsA-201 cells were performed as described previously [28] with minor modifications.

Living cells were incubated with 0.9 mg/ml Sulf-NHS-LC-LC-Biotin dissolved in water for 30 min at 4 °C. The reaction was quenched by incubating the cells with 10 mM Tris, pH 7.4, 150 mM NaCl for 30 min at 4 °C. Thereafter, the cells were harvested, incubated for 60 min at RT in lysis buffer (50 mM Hepes pH 7.4; 140 mM NaCl; 10% v/v Glycerol; 1% v/v Triton X-100; 1 mM EDTA; 2 mM EGTA, 0.5% deoxycholate and protease inhibitors) and centrifuged 15 min at 15,000 ×*g*. For each independent experiment the protein concentration was determined by the Nanodrop method. Supernatant was incubated overnight at 4 °C with streptavidin magnetic beads. The precipitated material was eluted in Laemmli buffer, run on SDS-PAGE minigels and blotted on PVDF membrane. The membrane was then split and subjected to Western blotting analysis with rabbit anti-TRPV1 (0.1 μg/ml), rabbit anti-Na^+/K^+ ATPase α1 (1:1000), and anti-GAPDH-hrp antibodies (1:10,000). GAPDH was used as an internal loading control for the total protein lysates, while Na^+/K^+ channel protein served as a loading control for the surface protein fraction. A rectangular region of interest was drawn in a way to include all TRPV1 glycosylation products (90 kDa and 105–110 kDa bands). The resulting density value was then normalized according to the density of the loading controls (GAPDH or Na^+/K^+). FujiFilm Las-1000 was used for image acquisition, NIH-ImageJ for image densitometry.

3. Results

3.1. Mass spectrometry analysis shows that Kvβ2 is specifically immunoprecipitated in association with TRPV1 channels

Previous studies indicated that TRPV1 channels are organized, like many other ion channels, in multiprotein signaling complexes [9–15]. In order to identify novel components of native TRPV1 channels, we embarked on a so far unexplored and rigorous biochemical approach of detergent-solubilizing TRPV1 channels from mouse DRG membranes, isolating the complex by immunoprecipitation and sequencing the harvested material by mass spectrometry. Initial experiments focused to establish the precise conditions of detergent solubilization. We aimed to optimize high solubilization efficiency of TRPV1 protein thereby using fairly mild solubilization conditions. A number of different detergents (lauroylsarcosine, digitonin, CHAPS, Triton X-100, SDS) and experimental conditions (incubation time, temperature, detergent concentration and protein:detergent ratio) were screened. Dodecanoyl sucrose was chosen as it performed best in our solubilization assay resulting in nearly quantitative solubilization of membrane protein as determined by Western blotting (Supplemental Fig. 1). This detergent is fairly mild (large, non-polar head group and a C_{12} aliphatic tail) with a low critical micelle concentration (CMC 0.30 mM), and is expected to show good preservation of the native molecular environment of an ion channel. We also set out to optimize our immunoprecipitation approach with respect to ionic strength and incubation time, using Western blotting experiments as read-out. Parallel experiments utilizing DRG from $TRPV1^{-/-}$ deficient animals served as negative controls. Under these conditions TRPV1 channels were quantitatively immunoprecipitated as the remaining supernatant was virtually devoid of TRPV1 channel protein (Fig. 1).

After having established suitable solubilization and immunoprecipitation conditions, membranes derived from approximately 100 mouse DRG were dodecanoyl sucrose-solubilized and immunoprecipitated as described under Experimental procedures. The immunoprecipitated material was quantitatively recovered from the antibody matrix after SDS denaturation. As a high concentration of SDS would have precluded subsequent trypsinization of the precipitated material, excess SDS was removed by gel electrophoresis, the isolated material was in-gel trypsinized, and the resulting peptide-fragments were analyzed by mass spectrometry. Several stringent criteria were adopted to minimize the occurrence of false-positive candidates: firstly, parallel experiments were performed using DRG membranes from $TRPV1^{-/-}$ deficient mice. Tryptic peptide fragments corresponding to proteins that were also detected in $TRPV1^{-/-}$ samples were excluded from further analysis. Secondly, every peptide ascribed to the IgG family was excluded from further analysis, as well as any peptide deriving from either trypsin autodigestion or keratins. Thirdly, proteins that were identified by less than two peptides were not taken into further account. The list of proteins resulting from mass spectrometric sequencing is shown in Table 1. Out of this list of potential TRPV1 interaction partners (Table 1), two proteins attracted our attention. TRPV2 protein was identified with high consistency, in accordance with previously published data [12,14], strengthening the validity of our approach. In addition, Kvβ2 was also consistently immunoprecipitated together with TRPV1 channel. By itself, we considered this finding quite remarkable as this protein was so far only characterized of being intimately associated with a number of voltage-gated potassium channels of the Kv1 family [17,18]. This result suggested that Kvβ2 could serve to be integral component of the TRPV1-associated protein complex probably accounting for discrete functional properties of native TRPV1 channels, and prompted us to further characterization.

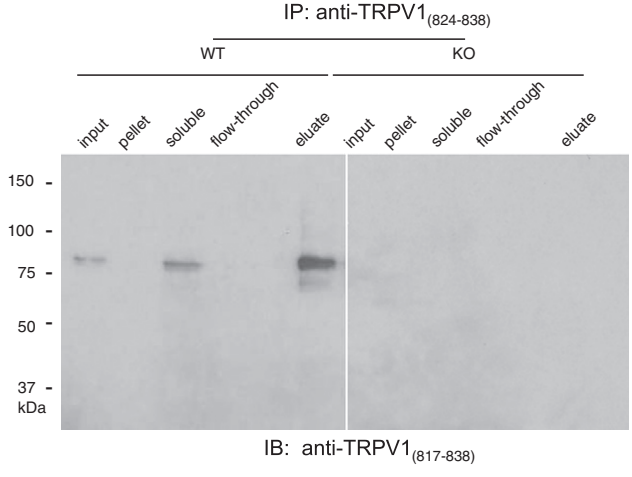

Fig. 1. Immunoprecipitation of TRPV1 protein. Western blotting of TRPV1 immunoprecipitation from solubilized mouse DRG membrane fraction with anti-$TRPV1_{(824–838)}$ antibody, monitored with anti-$TRPV1_{(817–838)}$ antibody. Parallel experiments were run with immunoprecipitated material from WT and the $TRPV1^{-/-}$ (KO) mice. For each condition, the following fractions were loaded on a gel: DRG membrane (input), non-soluble (pellet) and solubilized (soluble), non-bound material (flow-through) and eluate.

3.2. TRPV1 and Kvβ2 co-assemble after recombinant expression

In order to confirm that Kvβ2 protein is an interaction partner of TRPV1 channels, the two proteins were co-expressed in tsA-201 cells

Table 1
Proteins identified by mass spectrometry sequencing of the material precipitated in association with TRPV1 protein, and associated Mascot score. All proteins depicted were only found in wild-type samples. The presence of a tryptic peptide fragment in a $TRPV1^{-/-}$ sample resulted in exclusion of the protein for further analysis.

Protein	Accession number	Mascot score
TRPV1	gi47825364	1356
TRPV2	gi134053865	276
Kvβ2	gi975314	103
Actin	gi30425250	121
Rab-8B	gi27734154	78
Apolipoprotein O	gi81906185	88
Glycogen phosphorylase	gi6755256	51
Alpha-fodrin	gi930145	130
Cadherin 1	gi6753374	85
Zonula occludens protein 1	gi732430	85
U1 snRNP	gi67846113	59
Ribosomal protein L9	gi687604	108
Glucose 6 phosphatase	gi28395061	111

[20]. We reasoned that over-expressing these two proteins by recombinant means should allow stable complex formation which then could be verified by co-immunoprecipitation. TsA-201 cells were transiently transfected with plasmids encoding the cDNA sequences of TRPV1 and *myc*-tagged Kvβ2. Co-immunostaining experiments reveal a large degree of colocalization of both proteins (Supplemental Fig. 2). Neither TRPV1 nor Kvβ2 was detected in control mock-transfected cells, indicating that this expression system is largely devoid of these proteins. Western blots served as read-outs after detergent solubilization and immunoprecipitation. As shown in Fig. 2A, material precipitated by the anti-*myc* antibody (which will react with Kvβ2) contained Kvβ2 protein as well as significant amounts of TRPV1 protein. Conversely, our anti-TRPV1 antibodies precipitated also Kvβ2 material. Protein extracts of cells solely transfected with either TRPV1 or *myc*-Kvβ2 protein served as controls. Under these conditions, the respective antibodies did only precipitate their respective recombinant immunogenes, and did not display any cross-reactivity (Fig. 2B). These data demonstrate that TRPV1 and Kvβ2 are also capable to specifically co-assemble in vitro, in support of the mass spectrometry results obtained with DRG membranes.

Interestingly, Western blots of recombinant TRPV1 protein revealed a band pattern slightly different from native DRG TRPV1 protein. As

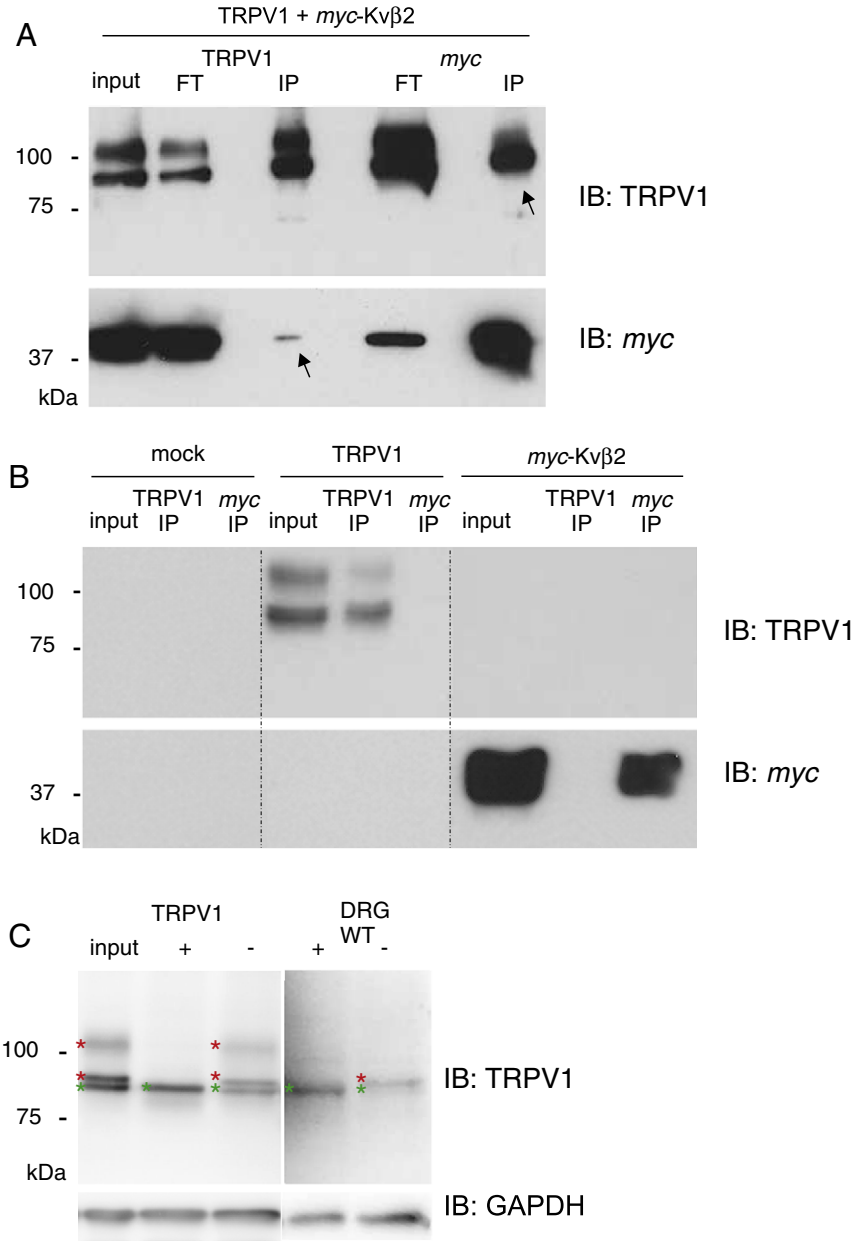

Fig. 2. TRPV1 and Kvβ2 co-immunoprecipitate when expressed together in tSA-201 cells. Starting material (input) and immunoprecipitated material with anti-TRPV1 and anti-*myc* antibodies were monitored with both, anti-TRPV1 and anti-*myc*, after 9% acrylamide gel electrophoretic separation. In each panel, top part was revealed with anti-TRPV1 antibody, bottom part with anti-*myc* antibody. Panel A shows double-transfected cells. Black arrows indicate co-immunoprecipitation signals: TRPV1 signal present in the material precipitated with anti-*myc* antibody (top), and *myc*-Kvβ2 band in the material precipitated with anti-TRPV1 antibody (bottom). Panel B shows specificity controls: cells transfected with mock empty plasmid (left), TRPV1 protein (middle) and *myc*-tagged Kvβ2 protein (right). FT: flow-through. Panel C: Western blots of membrane protein extracts from either TRPV1 protein after expression in tsA-201 cells (left), or from mouse DRG (right) are shown. For each condition, membrane lysates (input), treated with N-glycanase enzyme (+), or incubated in absence of the enzyme (−) were loaded on the gel. Each PVDF membrane was cut horizontally and monitored with anti-TRPV1$_{(817–838)}$ and anti-GAPDH antibodies. Red asterisk indicates glycosylated TRPV1 signal, green asterisk indicates non-glycosylated TRPV1. Western blotting detection was performed using a digital Peqlab imager.

shown in Fig. 2, a band of higher molecular weight (~105–110 kDa) is visible in addition to the expected size of TRPV1 protein (90 kDa). We considered this 105 kDa band to reflect TRPV1 protein with a higher degree of N-linked glycosylation in accordance with previous expression studies in HEK293 and in DRG-derived F11 cell lines [29]. In order to test this hypothesis, we carried out deglycosylation studies. As shown in Fig. 2C, enzymatic digestion of protein lysates with N-glycanase resulted in a molecular weight shift of TRPV1 protein in both, native and recombinant channels. After deglycosylation, only a 90 kDa band (green asterisk) was present indicating that the higher molecular weight bands are actually TRPV1 protein glycosylation products (red asterisk).

3.3. TRPV1 and Kvβ2 co-distribute in DRG neurons in primary culture

In order to investigate the co-distribution of TRPV1 and Kvβ2 protein in native neurons, we stained dissociated DRG neurons with the respective anti-TRPV1 and anti-Kvβ2 antibodies, and monitored antibody

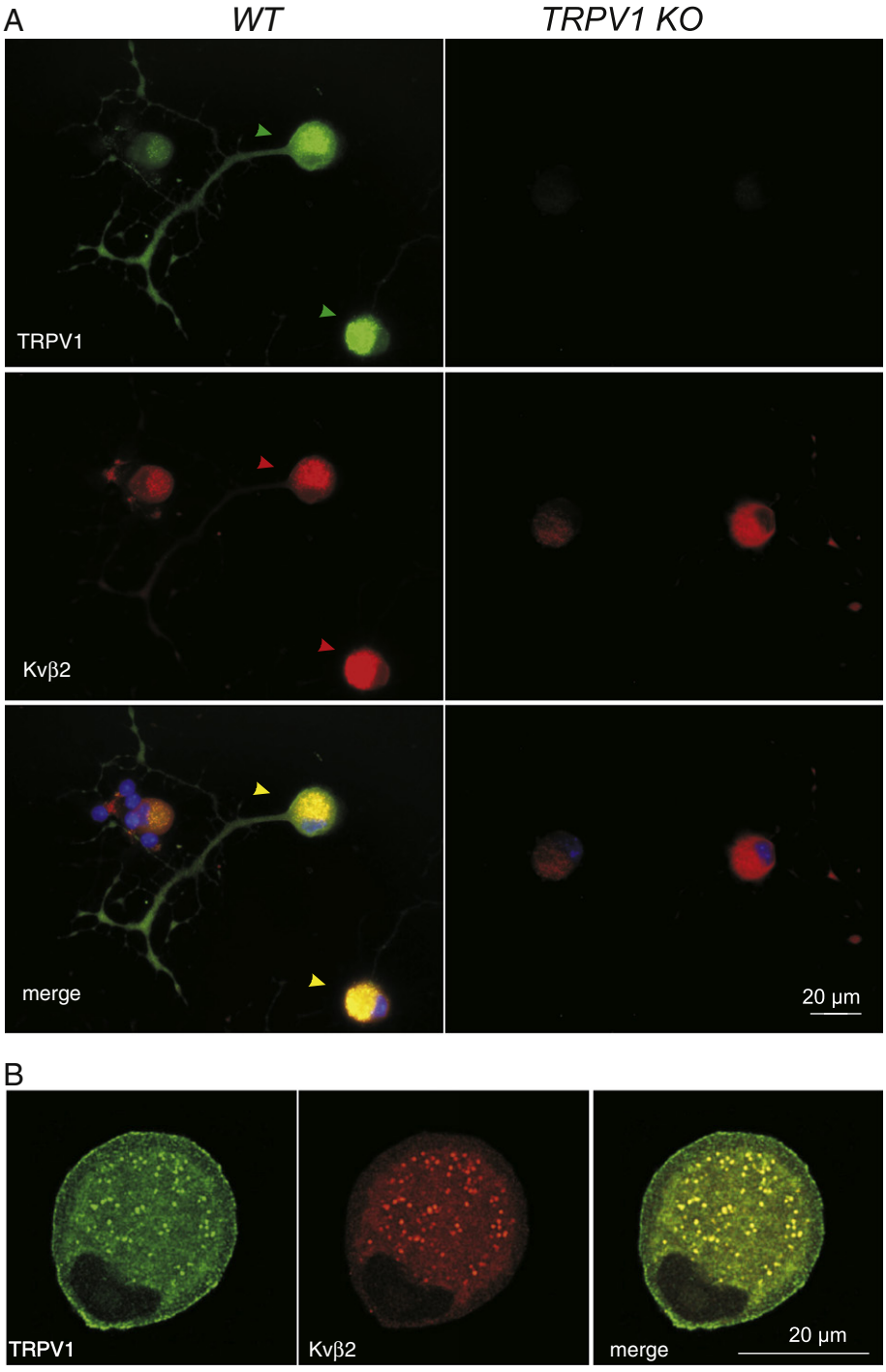

Fig. 3. Double immunostaining of TRPV1 and Kvβ2 in cultured sensor neurons. Panel A: representative picture of conventional fluorescence immunostaining of 24 h DRG neuron culture from WT (left) and TRPV1 KO (right) mice. TRPV1 (green) staining indicates positive neurons in WT neurons, while only background staining is detected in TRPV1 KO cultures. Kvβ2 staining (red) does not show substantial difference between WT and TRPV1 KO. In merge panel, neurons co-expressing TRPV1 and Kvβ2 are shown. Cell nuclei are stained in blue, arrowheads indicate co-expressing neurons. Panel B: One example of nucleus-level slice of confocal z-stack of WT mouse DRG neuron.

staining by immunofluorescence microscopy (Fig. 3A). Neuronal cultures of TRPV1$^{-/-}$ deficient mice were used as specificity controls. In accordance with previous studies [30], TRPV1 was observed mostly in small DRG neurons (18–30 μm), with an average diameter of 24.3 ± 7.9 μm (mean value ± SD, N = 4, n = 226). Out of all inspected neurons, 47.1 ± 8.9% displayed expression of TRPV1 immunoreactivity, while 38.5 ± 16.6% were positive for Kvβ2 staining. Moreover, 63.5 ± 20.7% of the neurons presenting TRPV1 immunoreactivity were also found to co-stain for Kvβ2 protein. Conversely, approximately 78.5 ± 7.1% of Kvβ2 expressing neurons were also positive for TRPV1 protein staining. This finding indicates that approximately 30.4% of DRG neurons do co-express both proteins under our experimental conditions.

In order to visualize the distribution of TRPV1 protein and Kvβ2 protein at higher spatial resolution, we performed confocal immunofluorescence microscopy. As shown in Fig. 3B, discrete co-localizing vesicles were observed in the cytoplasm, presumably representing newly synthesized channel subunits located in the ER/golgi compartment. In addition, TRPV1 immunoreactivity was also detected in the plasma membrane. Taken together, these data indicate that TRPV1 and Kvβ2 proteins are co-expressed in a subpopulation of sensory neurons, and show discrete co-localization towards vesicle-like entities presumably associated with endomembranes.

3.4. Kvβ2 protein increases cell surface expression of TRPV1 channel

Earlier studies established the Kvβ2 subunit to exert chaperone-like effects on various Kvα subunits, resulting in increase of cell surface expression [18,31–33]. Thus, we reasoned that Kvβ2 protein could contribute to increase cell surface expression of TRPV1 channel protein. In order to address this question, we performed cell surface biotinylation assays in the absence and presence of co-expressed Kvβ2 protein and monitored the level of biotinylated TRPV1 protein by means of Western blotting. GAPDH served as a loading control. As shown in Fig. 4A, Kvβ2 co-expression did not influence the TRPV1 protein overall expression levels. However, isolating the biotinylated surface protein fraction by streptavidin affinity chromatography indicated a 2.5 ± 0.6-fold increase (mean ± sem) of TRPV1 protein residing at the cell surface membrane after co-expression of Kvβ2 (Fig. 4B, C). As GAPDH was absent in the cell surface protein fraction (indicating assay specificity), monitoring of Na^+/K^+ ATPase served as loading control for the biotinylated surface fraction. These results suggest that Kvβ2 subunit is likely to play a chaperon-like role on TRPV1 protein, perhaps facilitating the trafficking of the ion channel to the cell surface.

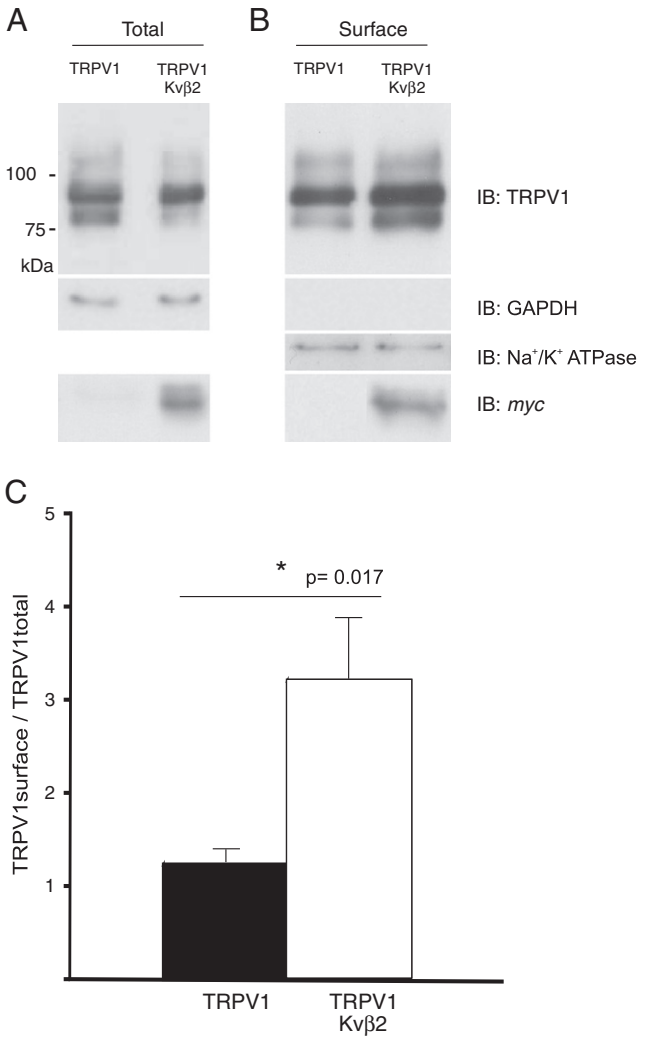

Fig. 4. Biotinylation of surface membrane proteins shows an increase of TRPV1 protein expression at the cell surface in presence of Kvβ2. Western blotting of TRPV1 protein in total lysate (Panel A) and biotinylated surface fraction (Panel B) of cells expressing solely TRPV1 protein or TRPV1 and Kvβ2. GAPDH served as loading control for the total lysate, Na^+/K^+ ATPase was used for the surface membrane protein fraction. Panel C: the increase of TRPV1 protein cell surface expression in presence of Kvβ2 is expressed as a ratio between the amount of TRPV1 protein detected at the cell surface and in the total lysate ($TRPV1_{surface}/TRPV1_{total}$). *P* value indicates statistical significance after Student's one tailed *t*-test, N = 4. Error bars indicate standard error of the mean.

3.5. Functional characterization of the TRPV1-Kvβ2 complex

After having established Kvβ2 protein to serve as an interaction partner of TRPV1 channels, we next investigated the functional implication of this interaction. We addressed this question by means of patch clamp studies recording capsaicin-activated currents (Icaps) in N1E-115-1 cells, as previously published [21,26,27], after heterologous expression of TRPV1 cDNA in the absence or presence of Kvβ2 cDNA. Capsaicin activation of TRPV1 channels expressed in N1E-115-1 cells resulted in the expected outward rectifying IV-relationship, as shown in Supplemental Fig. 3, which is indicative of activation of the non-specific cation channel TRPV1. In order to minimize capsaicin-dependent desensitization due to prolonged capsaicin exposure, we addressed the capsaicin dose dependency by applying a ramp-shaped depolarization from −100 mV to +100 mV. Capsaicin activated TRPV1 channels expressed in N1E-115-1 cells with an EC_{50} of 156.62 ± 21.51 nM (mean ± sem, n = 9) at −60 mV (Fig. 5B). At this negative voltage, capsaicin (1 μM) activated an inward current of −9.780 ± 0.512 nA, which did not further increase at higher capsaicin concentrations (Fig. 5A). At positive voltage (+80 mV) the EC_{50} was 133.22 ± 17.91 nM and 1 μM capsaicin elicited a maximal outward current of 12.886 ± 0.725 nA (Fig. 5A and B).

When co-expressing TRPV1 together with Kvβ2 in N1E-115 cells, the Icaps at both negative and positive holding potentials at saturating capsaicin concentrations did not differ from N1E-115-1 cells expressing TRPV1 alone (at 1 μM: inward; −9.996 ± 0.621 nA and outward; 12.878 ± 0.819 nA, n = 12). Furthermore, the size (34.37 ± 2.19 pF vs. 39.65 ± 2.60 pF) and the current densities of TRPV1 alone or TRPV1-Kvβ2 expressing cells at saturating capsaicin (≥1 μM) concentrations were not significantly different (at 1 μM Capsaicin: at −60 mV; −291.10 ± 21.22 vs. 270.54 ± 32.11 pA/pF and at +80 mV; 386.15 ± 28.90 vs. 349.90 ± 43.06 pA/pF, Fig. 5).

Interestingly, the EC_{50} of the capsaicin dose response curves at both, −60 mV and +80 mV was significantly shifted to the left by co-expression of Kvβ2 (74.61 ± 8.37 and 62.79 ± 5.82 nM respectively, Fig. 5A and B) indicating an increased TRPV1 sensitivity for capsaicin in the presence of Kvβ2. Also, co-expression of Kvβ2 increased the slope of capsaicin dose–response curves of Icaps (Fig. 5B).

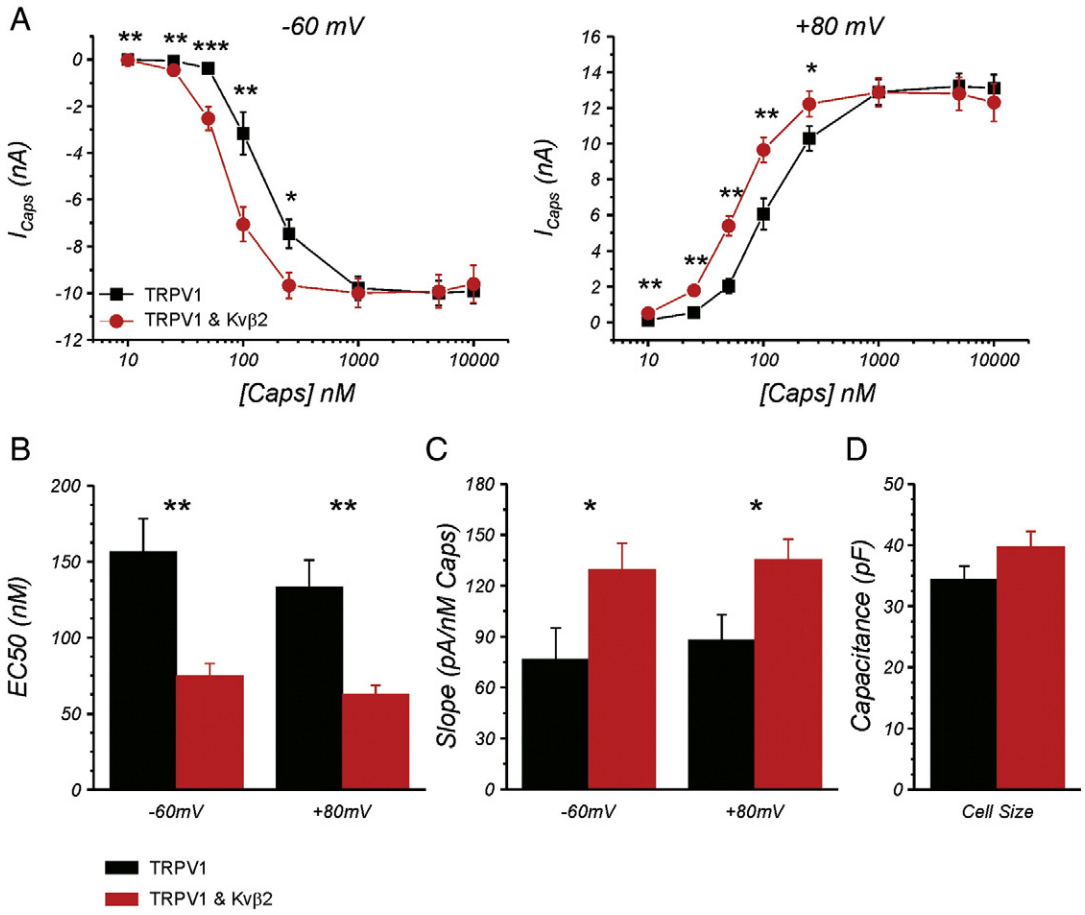

Fig. 5. Patch clamp recordings of capsaicin-activated currents in presence and in absence of Kvβ2. Panel A: dose response curve of TRPV1 capsaicin-activated inward current at −60 mV (left) and outward current at +80 mV (right) in presence (red circles) or in absence (black squares) of Kvβ2. The curve presents a decreased EC_{50} (Panel B) and increased slope (Panel C) in presence of Kvβ2, both at negative (−60 mV) and positive (+80 mV) potentials. Total capacitance does not change significantly (Panel D). Hill coefficients are as follows: −60 mV, TRPV1 = −2.2 ± 0.2, TRPV1 + Kvβ2 = −2.9 ± 0.2; +80 mV, TRPV1 = 1.8 ± 0.1, TRPV1 + Kvβ2 = 2.2 ± 0.2. Error bars indicate standard errors of the mean, $n = 9$, * stands for P value <0.05, ** stands for P value <0.01.

4. Discussion

4.1. Kvβ2 protein is associated with TRPV1 channel

Increasing evidence implies that TRPV1 channels are actively interacting with cellular proteins that modulate their activity and/or trafficking to the cell membrane [11,15,34]. The formation of such multi-protein complexes is expected to exert significant effects on the function of TRPV1 channels, as they could alter its gating and activation threshold. Thus, the identification and characterization of novel interaction partners is essential for a full understanding of the physiology of this ion channel. In this project we have tackled this goal by a combined approach of detergent-solubilization of TRPV1 channels derived from mouse DRG, protein complex immunoprecipitation and component sequencing by mass spectrometry. We isolated Kvβ2 protein, a so far unknown component of the TRPV1 channel complex which tightly associates with TRPV1 protein in both, heterologous expression system and native DRG neurons, as evidenced by immunoprecipitation assays and immunocytochemical approaches. Our experiments identified a number of additional TRPV1 interaction partners (Table 1), among them TRPV2 channel subunits. TRPV2 channel protein is accepted of being capable to form functional heterotetramers with TRPV1 [12,14], a fact which draws additional validity for the experimental approach chosen. Surprisingly, we failed to provide a clear demonstration of some of the previously characterized association partners, such as protein kinase A anchoring protein 150 (AKAP150) [15] and Pirt [11]. The reason for this lack of detection is currently unknown; however, different detergent solubilization protocols could partly explain this discrepancy as Triton X 100 was used in all previous studies, while we employed dodecanoyl sucrose.

Kvβ2 protein was initially identified as an accessory subunit of different Kv1 channels (for a review see Pongs and Schwarz [16]). Two predominant functions have been proposed for ancillary subunits of voltage-gated K^+ channel. Firstly, Kvβ subunits significantly contribute to the maturation and cell membrane trafficking of the pore-forming Kv1 subunit [16,18,35]. Secondly, the association of Kv1 channels with Kvβ2 protein has a marked influence on their gating properties [17,36,37] as well as pharmacological profile [38,39]. We have addressed the question whether any of these established functions of Kvβ2 protein are conserved for TRPV1 channels. The analysis of the relative amount of TRPV1 channel expressed at the cell surface clearly indicates that Kvβ2 protein expression leads to an increased amount of TRPV1 channel residing at the plasma membrane. Our co-immunoprecipitation data and the co-staining experiments in DRG neuron indicate an intimate – if not direct – interaction of the two proteins, and point towards the involvement of Kvβ2 protein in the transport of TRPV1 channel to the plasma membrane. This role could be partly similar for what was described by Shi et al. [18], who elucidated how Kvβ2 protein facilitates the trafficking of Kv1.2 channel to the cell membrane. As the subunit interaction domain in Shaker-type Kv1 channels was established by Gulbis [40], we searched for sequence homologies between this ion channel family and TRPV1. However, we were unable

to reveal any significant sequence homologies suggesting that a different Kvβ2 binding site may be involved. In addition, we did not observe any Kvβ2-dependent modification in the glycosylation pattern of TRPV1 channel (data not shown), which was observed by Shi et al. for Kv1.2 channels [18].

We have also investigated the effect of Kvβ2 on the gating properties of TRPV1 channel by measuring capsaicin-mediated currents in the absence or in the presence of Kvβ2 subunit. Our data show that Kvβ2 subunit renders TRPV1 channel significantly more sensitive to capsaicin. Similar effects were previously demonstrated for the Kvβ2 subunit, as reports have also shown that this protein is capable of altering drug pharmacology of Kv channels [38,39]. As an explanation for this effect, Kvβ2 protein could induce an allosteric change in the TRPV1 tri-dimensional conformation, resulting in an increased response to capsaicin. However, our patch-clamp recordings do not reveal an increase in capsaicin-mediated current density accompanying the increase in the cell surface expression of TRPV1 channel. This observation could be explained by the fact that the increased number of TRPV1 channel exposed at the cell surface of transfected cells might not necessarily reflect a pool of fully functional TRPV1 homotetramers. Similar effects were observed in heterologous TRPV1 expression studies [34,36,41,42]. Lilja et al. have shown in TRPV1 expressing SH-SY5Y cells that TRPV1 surface expression was increased in insulin- and IGF-I-treated cells compared to untreated, and EC_{50} values also were lowered, indicative of a sensitization [42]. However, similar to what we observe in our present study, the maximal response in Ca^{2+} influx was not significantly increased in insulin- and IGF-I-treated cells. Plausibly, this might also be the case for Kvβ2-mediated sensitization, although mechanistic explanation of the observed results will have to await further experiments.

4.2. Kvβ2 as a molecular scaffold?

Kvβ2 could also serve a novel yet unidentified role in the TRPV1 channel complex. As Kvβ2 appears to possess high affinity for both, voltage-gated K^+ channels as well as TRPV1, it seemed feasible that it may serve an interaction scaffold between these two ion channels bringing them in close spatial proximity. Kv1.4 appears to be the prime candidate for such a multichannel complex, as it was previously shown to be highly expressed in small diameter DRG neurons [43] and, more importantly, to form a stable complex with Kvβ2 [44,45]. Such Kv1.4/TRPV1/Kvβ2 complex would be expected to assemble in the ER-Golgi compartment, and to be subsequently transported to axonal termini, where both, TRPV1 and Kv1.4 channels were previously shown to be targeted to [43]. A similar function of Kvβ2 was previously demonstrated for Kv1.2 [31,46], which is also detected in the axonal compartments (e.g. juxtaparanode or cerebellar Pinceau terminals [47,48]).

What might be the functional implication of such a putative ion channel complex? This ion channel assembly could provide a structural basis of a rapid hence spatially restricted repolarization pathway. A depolarizing Na^+/Ca^{2+} influx through TRPV1 channel would be counteracted by a fast repolarizing K^+ efflux through Kv1.4 channels. Despite significant experimental effort, we could not demonstrate this interaction by means of immunoprecipitation and subsequent Western blotting or mass spectrometric protein sequencing because of its non-existence, or, if existing, a very subtle and transient interaction, which was weakened by the solubilization protocol employed. However, additional experiments will certainly address this yet unexplored question in further detail.

4.3. Possible role of Kvβ2 as a redox sensor?

An alternative role for Kvβ2 protein could be its function as oxygen sensor. Kvβ2 was previously shown to belong to the aldo-keto-reductase superfamily, and was demonstrated to display an enzymatic redox activity in permanent association with NAPDH cofactor [49,50]. This redox reaction catalyzed by Kvβ2 affects Kv1 channel function, resulting in a decrease of the inactivating rate of the ion channel [50]. Therefore, Kvβ2 protein is often referred to as a redox sensor, being able modulate the activity of the channel in response to changes in the redox environment. Importantly, TRPV1 was shown to undergo redox modulation, eliciting stronger heat-activated currents in the presence of both reducing and oxidizing agents [51]. Taken together, these observations suggest that a possible interpretation for the functionality of the protein–protein interaction that we describe herein could be that Kvβ2 senses redox changes in cytoplasmic environment and transmits this information to the associated TRPV1 channel, which would in turn undergo conformational changes leading to increased heat sensitivity. Therefore, changes in the redox state in a variety of pathophysiological conditions, such as tissue damage and inflammation, might contribute to modulate TRPV1 activity and result in nociceptor sensitization.

In summary, our results are consistent with the notion that Kvβ2 subunit is a novel interaction partner of TRPV1 protein in mouse DRG. In vitro data suggest for Kvβ2 a chaperon-like role on TRPV1 channels, increasing their surface expression, as well as a sensitizing effect of TRPV1 channels in response to capsaicin. This subunit association could also be involved in proper TRPV1 channels targeting to axonal compartments, although additional work is required to reveal the effect of such interaction in vivo.

Supplementary data to this article can be found online at http://dx.doi.org/10.1016/j.bbamcr.2013.09.001.

Acknowledgements

We thank Alexandra Koschak for providing us tsA-201 cells and Francesco Ferraguti for sharing his anti-Na^+/K^+ ATPase α1 antibody with us. We also thank Sandra Santos Sierra for constructive discussion, Georg Wietzorrek for $TRPV1^{-/-}$ mice genotyping and the Biooptics facility of the Medical University Innsbruck for technical support.

References

[1] M.J. Caterina, M.A. Schumacher, M. Tominaga, T.A. Rosen, J.D. Levine, D. Julius, The capsaicin receptor: a heat-activated ion channel in the pain pathway, Nature 389 (1997) 816–824.
[2] D.C. Immke, N.R. Gavva, The TRPV1 receptor and nociception, Semin. Cell Dev. Biol. 17 (2006) 582–591.
[3] J.B. Davis, J. Gray, M.J. Gunthorpe, J.P. Hatcher, P.T. Davey, P. Overend, M.H. Harries, J. Latcham, C. Clapham, K. Atkinson, S.A. Hughes, K. Rance, E. Grau, A.J. Harper, P.L. Pugh, D.C. Rogers, S. Bingham, A. Randall, S.A. Sheardown, Vanilloid receptor-1 is essential for inflammatory thermal hyperalgesia, Nature 405 (2000) 183–187.
[4] D.E. Clapham, L.W. Runnels, C. Strübing, The TRP ion channel family, Nat. Rev. Neurosci. 2 (2001) 387–396.
[5] I.B. Levitan, Signaling protein complexes associated with neuronal ion channels, Nat. Neurosci. 9 (2006) 305–310.
[6] H. Husi, M.A. Ward, J.S. Choudhary, W.P. Blackstock, S.G. Grant, Proteomic analysis of NMDA receptor–adhesion protein signaling complexes, Nat. Neurosci. 3 (2000) 661–669.
[7] C.S. Müller, A. Haupt, W. Bildl, J. Schindler, H.G. Knaus, M. Meissner, B. Rammner, J. Striessnig, V. Flockerzi, B. Fakler, U. Schulte, Quantitative proteomics of the Cav2 channel nano-environments in the mammalian brain, Proc. Natl. Acad. Sci. U. S. A. 107 (2010) 14950–14957.
[8] J.S. Shin, M.H. Wang, S.W. Hwang, H. Cho, S.Y. Cho, M.J. Kwon, S.Y. Lee, U. Oh, Differences in sensitivity of vanilloid receptor 1 transfected to human embryonic kidney cells and capsaicin-activated channels in cultured rat dorsal root ganglion neurons to capsaicin receptor agonists, Neurosci. Lett. 16 (2001) 135–139.
[9] C. Goswami, M. Dreger, R. Jahnel, O. Bogen, C. Gillen, F. Hucho, Identification and characterization of a Ca^{2+}-sensitive interaction of the vanilloid receptor TRPV1 with tubulin, J. Neurochem. 91 (2004) 1092–1103.
[10] C. Goswami, M. Dreger, H. Otto, B. Schwappach, F. Hucho, Rapid disassembly of dynamic microtubules upon activation of the capsaicin receptor TRPV1, J. Neurochem. 96 (2006) 254–266.
[11] A.Y. Kim, Z. Tang, Q. Liu, K.N. Patel, D. Maag, Y. Geng, X. Dong, Pirt, a phosphoinositide-binding protein, functions as a regulatory subunit of TRPV1, Cell 133 (2008) 475–485.
[12] A. Liapi, J.N. Wood, Extensive co-localization and heteromultimer formation of the vanilloid receptor-like protein TRPV2 and the capsaicin receptor TRPV1 in the adult rat cerebral cortex, Eur. J. Neurosci. 22 (2005) 825–834.
[13] C. Morenilla-Palao, R. Planells-Cases, N. Garcia-Sanz, A. Ferrer-Montiel, Regulated exocytosis contributes to protein kinase C potentiation of vanilloid receptor activity, J. Biol. Chem. 279 (2004) 25665–25672.

[14] A.R. Rutter, Q.P. Ma, M. Leveridge, T.P. Bonnert, Heteromerization and colocalization of TrpV1 and TrpV2 in mammalian cell lines and rat dorsal root ganglia, Neuroreport 16 (2005) 1735–1739.
[15] X. Zhang, L. Li, P.A. McNaughton, Proinflammatory mediators modulate the heat-activated ion channel TRPV1 via the scaffolding protein AKAP79/150, Neuron 59 (2008) 450–461.
[16] O. Pongs, J.R. Schwarz, Ancillary subunits associated with voltage-dependent K^+ channels, Physiol. Rev. 90 (2010) 755–797.
[17] K. McCormack, T. McCormack, M. Tanouye, B. Rudy, W. Stühmer, Alternative splicing of the human Shaker K^+ channel beta1 gene and functional expression of the beta2 gene product, FEBS Lett. 370 (1995) 32–36.
[18] G. Shi, K. Nakahira, S. Hammond, K.J. Rhodes, L.E. Schechter, J.S. Trimmer, Beta subunits promote K channel surface expression through effects early in biosynthesis, Neuron 16 (1996) 863–872.
[19] H.G. Knaus, A. Eberhart, R.O. Koch, P. Munujos, W.A. Schmalhofer, J.W. Warmke, G.J. Kaczorowski, M.L. Garcia, Characterization of tissue-expressed alpha subunits of the high conductance Ca(2+)-activated K^+ channel, J. Biol. Chem. 270 (1995) 22434–22439.
[20] A. Singh, D. Hamedinger, J.C. Hoda, M. Gebhart, A. Koschak, C. Romanin, J. Striessnig, C-terminal modulator controls Ca^{2+}-dependent gating of Ca(v)1.4 L-type Ca^{2+} channels, Nat. Neurosci. 9 (2006) 1108–1116.
[21] T. Amano, E. Richelson, M. Nirenberg, Neurotransmitter synthesis by neuroblastoma clones (neuroblast differentiation–cell culture–choline acetyltransferase–acetylcholinesterase–tyrosine hydroxylase–axons–dendrites), Proc. Natl. Acad. Sci. U. S. A. 69 (1972) 258–263.
[22] H. Berkefeld, C.A. Sailer, W. Bildl, V. Rohde, J.O. Thumfart, S. Eble, N. Klugbauer, E. Reisinger, J. Bischofberger, D. Oliver, H.G. Knaus, U. Schulte, B. Fakler, BKCa-Cav channel complexes mediate rapid and localized Ca^{2+}-activated K^+ signaling, Science 314 (2006) 615–620.
[23] C. Winkler, K. Denker, S. Wortelkamp, A. Sickmann, Silver- and Coomassie-staining protocols: detection limits and compatibility with ESI MS, Electrophoresis 28 (2007) 2095–2099.
[24] A. Shevchenko, M. Wilm, O. Vorm, M. Mann, Mass spectrometric sequencing of proteINS silver-stained polyacrylamide gels, Anal. Chem. 68 (1996) 850–858.
[25] M. Andratsch, N. Mair, C.E. Constantin, N. Scherbakov, C. Benetti, S. Quarta, C. Vogl, C.A. Sailer, N. Uceyler, J. Brockhaus, R. Martini, C. Sommer, H.U. Zeilhofer, W. Muller, R. Kuner, J.B. Davis, S. Rose-John, M. Kress, A key role for gp130 expressed on peripheral sensory nerves in pathological pain, J. Neurosci. 29 (2009) 13473–13483.
[26] M. Langeslag, C.E. Constantin, M. Andratsch, S. Quarta, N. Mair, M. Kress, Oncostatin M induces heat hypersensitivity by gp130-dependent sensitization of TRPV1 in sensory neurons, Mol. Pain 7 (2011) 102–111.
[27] N. Mair, C. Benetti, M. Andratsch, M.G. Leitner, C.E. Constantin, M. Camprubí-Robles, S. Quarta, W. Biasio, R. Kuner, I.L. Gibbins, M. Kress, R.V. Haberberger, Genetic evidence for involvement of neuronally expressed S1P receptor in nociceptor sensitization and inflammatory pain, PLoS One 3 (2011) 17268–17279.
[28] W. Wong, E.W. Newell, D.G. Jugloff, O.T. Jones, L.C. Schlichter, Cell surface targeting and clustering interactions between heterologously expressed PSD-95 and the Shal voltage-gated potassium channel, Kv4.2, J. Biol. Chem. 277 (2002) 20423–20430.
[29] R. Jahnel, M. Dreger, C. Gillen, O. Bender, J. Kurreck, F. Hucho, Biochemical characterization of the vanilloid receptor 1 expressed in a dorsal root ganglia derived cell line, Eur. J. Biochem. 268 (2001) 5489–5496.
[30] A. Guo, L. Vulchanova, J. Wang, X. Li, R. Elde, Immunocytochemical localization of the vanilloid receptor 1 (VR1): relationship to neuropeptides, the P2X3 purinoceptor and IB4 binding sites, Eur. J. Neurosci. 11 (1999) 946–958.
[31] C. Gu, Y.N. Jan, L.Y. Jan, A conserved domain in axonal targeting of Kv1 (Shaker) voltage-gated potassium channels, Science 301 (2003) 646–649.
[32] C. Gu, W. Zhou, M.A. Puthenveedu, M. Xu, Y.N. Jan, L.Y. Jan, The microtubule plus-end tracking protein EB1 is required for Kv1 voltage-gated K^+ channel axonal targeting, Neuron 52 (2006) 803–816.
[33] H. Vacher, J.W. Yang, O. Cerda, A. Autillo-Touati, B. Dargent, J.S. Trimmer, Cdk-mediated phosphorylation of the Kvbeta2 auxiliary subunit regulates Kv1 channel axonal targeting, J. Cell Biol. 192 (2011) 813–824.
[34] S. Lainez, P. Valente, I. Ontoria-Oviedo, J. Estevez-Herrera, M. Camprubi-Robles, A. Ferrer-Montiel, R. Planells-Cases, GABAA receptor associated protein (GABARAP) modulates TRPV1 expression and channel function and desensitization, FASEB J. 24 (2010) 1958–1970.
[35] C.R. Campomanes, K.I. Carroll, L.N. Manganas, M.E. Hershberger, B. Gong, D.E. Antonucci, K.J. Rhodes, J.S. Trimmer, Kv beta subunit oxidoreductase activity and Kv1 potassium channel trafficking, J. Biol. Chem. 277 (2002) 8298–8305.
[36] E.A. Accili, J. Kiehn, B.A. Wible, A.M. Brown, Interactions among inactivating and noninactivating Kvbeta subunits, and Kvalpha1.2, produce potassium currents with intermediate inactivation, J. Biol. Chem. 272 (1997) 28232–28236.
[37] K. McCormack, J.X. Connor, L. Zhou, L.L. Ho, B. Ganetzky, S.Y. Chiu, A. Messing, Genetic analysis of the mammalian K^+ channel beta subunit Kvbeta 2 (Kcnab2), J. Biol. Chem. 277 (2002) 13219–13228.
[38] J.P. Beekwilder, M.E. O'Leary, L.P. van den Broek, G.T. van Kempen, D.L. Ypey, R.J. van den Berg, Kv1.1 channels of dorsal root ganglion neurons are inhibited by n-butyl-p-aminobenzoate, a promising anesthetic for the treatment of chronic pain, J. Pharmacol. Exp. Ther. 304 (2003) 531–538.
[39] T. Gonzalez, R. Navarro-Polanco, C. Arias, R. Caballero, I. Moreno, E. Delpon, J. Tamargo, M.M. Tamkun, C. Valenzuela, Assembly with the Kvbeta1.3 subunit modulates drug block of hKv1.5 channels, Mol. Pharmacol. 62 (2002) 1456–1463.
[40] J.M. Gulbis, Structure of the cytoplasmic beta subunit–T1 assembly of voltage-dependent K^+ channels, Science 289 (2000) 123–127.
[41] T.K. Baumann, M.E. Martenson, Extracellular protons both increase the activity and reduce the conductance of capsaicin-gated channels, J. Neurosci. 20 (2000) RC80.
[42] J. Lilja, F. Laulund, A. Forsby, Insulin and insulin-like growth factor type-I up-regulate the vanilloid receptor-1 (TRPV1) in stably TRPV1-expressing SH-SY5Y neuroblastoma cells, J. Neurosci. Res. 85 (2007) 1413–1419.
[43] U. Binzen, W. Greffrath, S. Hennessy, M. Bausen, S. Saaler-Reinhardt, R.D. Treede, Co-expression of the voltage-gated potassium channel Kv1.4 with transient receptor potential channels (TRPV1 and TRPV2) and the cannabinoid receptor CB1 in rat dorsal root ganglion neurons, Neuroscience 142 (2006) 527–539.
[44] E.A. Accili, Y.A. Kuryshev, B.A. Wible, A.M. Brown, Separable effects of human Kvbeta1.2 N- and C-termini on inactivation and expression of human Kv1.4, J. Physiol. 512 (1998) 325–336.
[45] R. Peri, B.A. Wible, A.M. Brown, Mutations in the Kv beta 2 binding site for NADPH and their effects on Kv1.4, J. Biol. Chem. 276 (2001) 738–741.
[46] Y. Gu, C. Gu, Dynamics of Kv1 channel transport in axons, PLoS One 5 (2010) 11931–11940.
[47] E.J. Arroyo, Y.T. Xu, L. Zhou, A. Messing, E. Peles, S.Y. Chiu, S.S. Scherer, Myelinating Schwann cells determine the internodal localization of Kv1.1, Kv1.2, Kvbeta2, and Caspr, J. Neurocytol. 28 (1999) 333–347.
[48] A.P. Southan, B. Robertson, Patch-clamp recordings from cerebellar basket cell bodies and their presynaptic terminals reveal an asymmetric distribution of voltage-gated potassium channels, J. Neurosci. 18 (1998) 948–955.
[49] S. Mann, J.M. Gulbis, R. MacKinnon, Structure of voltage-dependent K^+ beta subunit, Cell 97 (1999) 10.
[50] J. Weng, Y. Cao, N. Moss, M. Zhou, Modulation of voltage-dependent Shaker family potassium channels by an aldo-keto reductase, J. Biol. Chem. 281 (2006) 15194–15200.
[51] K. Susankova, K. Tousova, L. Vyklicky, J. Teisinger, V. Vlachova, Reducing and oxidizing agents sensitize heat-activated vanilloid receptor (TRPV1) current, Mol. Pharmacol. 70 (2006) 383–394.